Radiation Processing and Characterization of Poly(vinyl alcohol) Nano-Composites, Part 1: Nano-Particulate Filler Tuned Crosslinking Behavior

Kumar A. Dubey,[1] Chandrasekhar V. Chaudhari,[1] Rekha Rao,[2] Yatender K. Bhardwaj,[1] Narender K. Goel,[1] Sunil Sabharwal[1]

[1]*Radiation Technology Development Division, Bhabha Atomic Research Center, Mumbai, Maharashtra 400 085, India*
[2]*Solid State Physics Division, Bhabha Atomic Research Center, Mumbai, Maharashtra 400 085, India*

Received 24 November 2009; accepted 25 April 2010
DOI 10.1002/app.32710
Published online 14 July 2010 in Wiley InterScience (www.interscience.wiley.com).

ABSTRACT: Nano-composites of poly vinyl alcohol containing different nano-fillers namely multiple walled carbon nanotubes (MWNT), single walled carbon nanotubes (SWNT), silica nanoparticles, and silver nanoparticles were prepared by sonication-assisted solution mixing and subjected to different doses of gamma radiation. The efficacy of radiation crosslinking was analyzed by sol–gel analysis, Charlesby-Pinner parameter estimation and crosslinking density measurements. Crosslinking of nano-composites was found to increase with radiation dose and markedly affected with the type of nano-particulate filler in the matrix (p_o/q_o in the range: 0.40–0.83). The results have been explained on the basis of Raman spectroscopy, hydrodynamic volume measurements, contact angle measurements, and scanning electron microscopy (SEM). © 2010 Wiley Periodicals, Inc. J Appl Polym Sci 118: 3490–3498, 2010

Key words: radiation; nanoparticles; crosslinking; poly(vinyl alcohol)

INTRODUCTION

Polymers are usually reinforced with carbon black, silica, and other microscopic fillers and further crosslinked by various means for the development of high performance material.[1–3] There is, however, an emerging interest in the development of radiation crosslinked polymer composites filled with nano-particulate fillers as, even if the nano-fillers are incorporated in minute quantity, such radiation processed polymer nano-composites have been envisaged to have superior physical and mechanical properties than their conventional analogs.[4–7]

High-energy ionizing radiations, mainly gamma and electron beam, have been widely used in the crosslinking of polymers primarily because of their efficiency to produce uniformly crosslinked networks in a wide range of polymers. The low operation cost, additive free technique, and room temperature operations are among the added advantages of radiation crosslinking over the existing crosslinking techniques.[8–12] There are many reports on the development of radiation processed polymer nano-composite material and the analysis of their mechanical and physical properties, however not much information is available on the radiation crosslinking behavior of such nano-composites with special reference to the nature, type, and concentration of nano-particulate filler present in the parent polymer matrix.

Poly(vinyl alcohol) (PVA) is an interesting polymer to study the effect of nano-particulate filler on its radiation crosslinking behavior as it has good radiation crosslinking yield G(X) and radiation processed PVA nano-composites have imminent practical interests in the development of implantable biomaterials and biodegradable plastics.[13,14] Moreover, though PVA and its blends have been widely modified and processed using high-energy radiation for various applications, not much work has been reported on the radiation effects on PVA reinforced with nanomaterials.[15–17] Optimally radiation crosslinked PVA nano-composites are expected to overcome the intrinsic structural weaknesses of PVA. Earlier studies have shown that addition of nano-particulate fillers does affect the radiation sensitivity of the parent matrix and there is disagreement among various workers on the gelation characteristic of filler reinforced polymers.[18,19] In the present work, we report a detailed investigation on the effect of nanoparticle addition on the radiation induced crosslinking behavior of PVA nano-composites. Attempts have been made to critically understand such effects in the light of various microscopic and

Correspondence to: Y. K. Bhardwaj (ykbhard@barc.gov.in).

TABLE I
Compositional Characteristics, Designations for Nano-Composites

Nano-particulate filler (5%)	Size (nm)	Sample designation
Nil	–	Bl
MWNT	10–15	MW
SWNT	2–5	SW
Silica	10	Si
Silver	20	Sv

macroscopic changes taking place in PVA on nano-composite formation as well as on irradiation.

EXPERIMENTAL

Materials

PVA (Mol wt. 125,000 LR grade) in powder form was procured from M/s Prabhat Chemicals, India and used as such. MWNT and SWNT powders from M/s Nanocyl; Belgium were used without further purification. Silica and silver nanoparticles were received from M/s Aldrich. Other properties of nano-particulate fillers used in the study have been provided in Table I. All other chemicals used were of analytical grade (Purity $>$ 99%). Double distilled water was used for preparation of all solutions and extraction of homopolymer.

Nano-composites preparation

Nano-composites of PVA with nanoparticles mentioned in Table I were prepared by initially mixing and stirring the 5% (w/v) aqueous solution of PVA with desired nanoparticles for 30 min followed by sonication for an hour and later casting on clean glass plates. The nano-composite compositions and sample designation have been represented in Table I.

Irradiation of samples

Irradiation was carried out under aerated condition using a gamma chamber 5000 (GC-5000) at 32 $\pm$ 1°C having Co-60 gamma source supplied by M/s BRIT, India. The dose rate of gamma chamber was ascertained to be 3.5 kGy h^{-1} by Fricke dosimetry prior to irradiation of samples.

Morphological studies

The surface morphology of the nano-composites were examined by a scanning electron microscope (SEM) using VEGA MV2300T/40 (TS 5130 MM) microscope (TESCAN) at an acceleration voltages of 30 kV and magnification range 200–10,000×. All surfaces were coated with a thin layer of gold under vacuum prior to SEM examination.

Dilute solution viscometry (DSV)

All the measurements for ternary or binary system were performed at 25°C (+0.1) using dilution Ubbelohde type capillary viscometer immersed in a constant temperature bath. The stock solutions of each ternary or binary systems were made by dissolving the appropriate amount of polymer in water (0.5 gdl^{-1}). Dilutions to yield at least six lower concentrations were made by adding appropriate aliquots of solvent. The elution time of each solution was determined as average of several readings.

Gel content

The gel content was determined by refluxing the samples with water for 24 h. The remaining insoluble portion was initially dried under room conditions and then in vacuum oven at 60°C to a constant weight. Gel content was evaluated using following relationship [eq. (1)], where W_g and W_i are the weight of insoluble fraction and initial weight, respectively

$$\text{Gel content} = \left(\frac{w_g}{w_i}\right) \quad (1)$$

Crosslink density measurements by solvent sorption measurement

For the crosslink density measurement, dried nano-composites gels obtained after extraction and drying were cut into cylindrical form (diameter $\sim$ 10 mm; thickness $\sim$ 1–3 mm) using a sharp edged die. Pre-weighed samples were placed in a 200-mesh stainless steel compartment and immersed in water. The water uptake was monitored gravimetrically by weighing the specimen till equilibrium weight was attained. The swelled samples were periodically removed, blotted free of surface water using laboratory tissue paper, weighed on AND analytical balance (accuracy 0.00001 g) in stopper bottles and returned to the swelling medium.

Raman spectroscopic studies

Raman spectra were excited using 532 nm line of diode pumped Nd-YAG laser of power 15 mW. Scattered light was analyzed using a home built 0.9 m single monochromator, coupled with a super notch filter and detected by a cooled CCD (Andor technology). Entrance slit was kept at 50 μm, which gives a spectral band pass of 3 cm^{-1}.

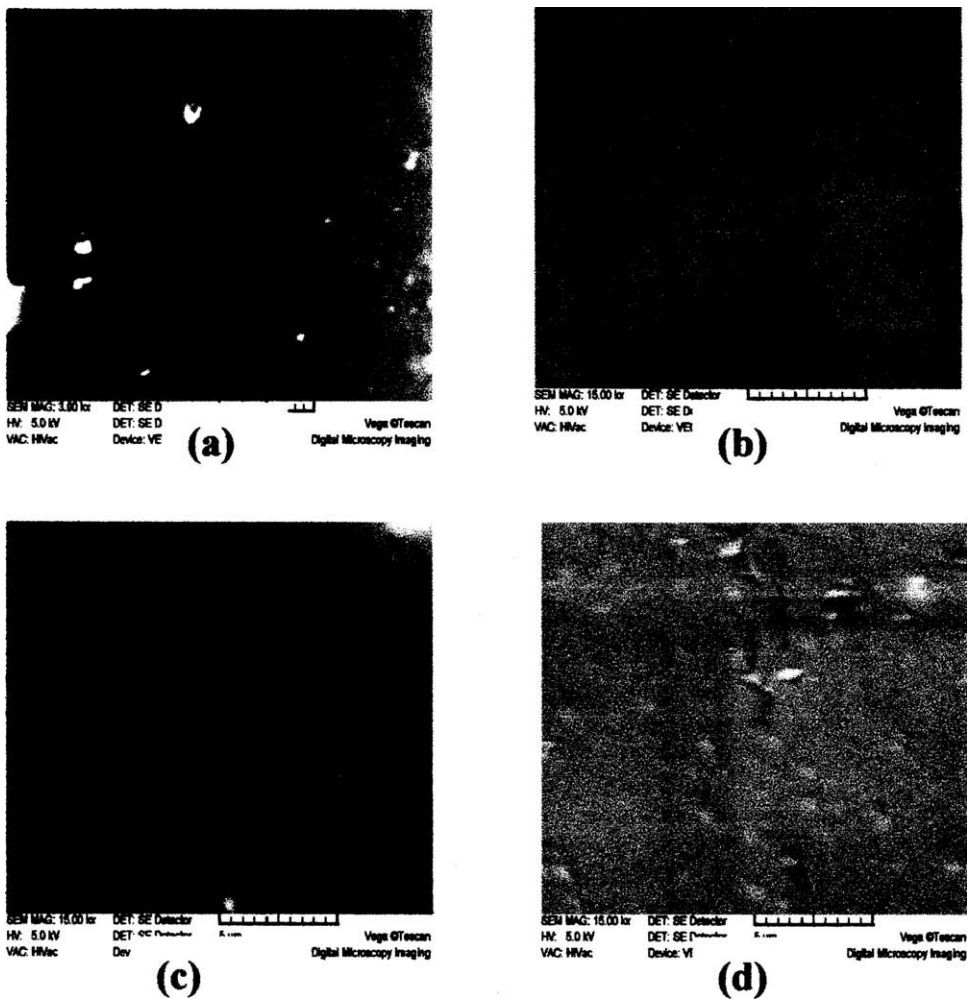

Figure 1 Scanning electron micrographs of PVA-nano-composites containing (a) MWNT, (b) Silica, (c) SWNT, and (d) Silver.

Contact angle measurements

Contact angle measurements of PVA-nanocomposites were performed by following the sessile drop method. A contact angle instrument from M/s GBX instruments, France equipped with image analysis software (Windrop^{++}, GBX instruments) was used for the purpose. A liquid droplet (1.5–2.5 μL) was allowed to fall on the samples to be studied from a software-controlled syringe. An image sequence was recorded through the CCD camera on a PC computer and interfaced to image capture software. Each reported data represents an average measured contact angle of at least three individual drops that were tested in different locations on a given blend film.

RESULTS

The scanning electron micrographs of fractured surfaces of PVA nano-composites (shown in Fig. 1) did not show any agglomeration of nano-particulate fillers indicating uniform dispersal of the fillers in the matrix.

The extent of radiation effects on PVA-nanocomposites in aqueous medium will be a function of many experimental variables such as dose, dose rate, type of nano-filler, polymer concentration, types and concentration of radiolytic products generated in the medium. Therefore, effect of some of these experimental parameters was studied in this part of study.

Effect of gamma radiation on nano-composites

Figure 2 shows the change in the gel content of PVA-nano-composites on irradiation. Un-irradiated samples were soluble in hot water, however nanocomposites irradiated to a dose >10 kGy were partly soluble due to the formation of a three-dimensional network. The gel fractions were found to reduce significantly with incorporation of nano-particulate fillers in the PVA matrix. The pure PVA showed gel fraction values between 0.76 and 0.90 in the dose range studied; whereas, the maximum gel fraction

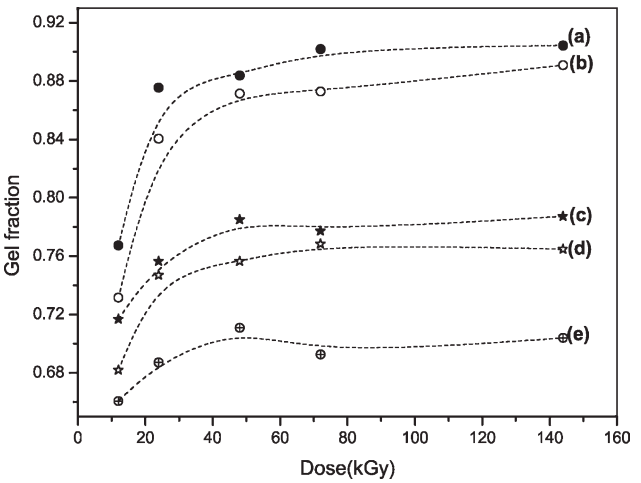

Figure 2 Gel fractions of PVA nano-composites on irradiation at a dose rate of 3.5 $kGyh^{-1}$ containing different nano-fillers (a) Blank, (b) Silica, (c) Silver, (d) SWNT, and (e) MWNT.

observed with MWNT nano-composite was less than 0.70 in the same dose range. At all doses, the gel fraction followed the sequence Blank > Silica > Silver > SWNT > MWNT.

To quantitatively evaluate crosslinking and chain scission yields of irradiated PVA nano-composites, plots of $S + S^{1/2}$ vs 1/radiation dose from the Charlesby-Pinner equation [eq. (2)] for the different nano-composites compositions were drawn (Fig. 2)[20,21]

$$S + \sqrt{S} = \frac{p_0}{q_0} + \frac{1}{q_0 P_n D} \tag{2}$$

where S is the sol fraction, P_n the number averaged degree of polymerization, D radiation dose, p_0 and q_0 are fraction of ruptured and crosslinked main-chain units per unit dose (proportional to the radiation chemical yields of degradation and crosslinking).

From Figure 3 and its inset figure, it is clear that pure PVA is most efficiently crosslinked on irradiation and the crosslinking extent decreased in the presence of nano-particulate fillers in the matrix.

Crosslinking density and density of radiation processed nano-composites

To gain insight into radiation-induced changes in PVA-nano-composites, crosslinking density measurements were carried out. The key parameters determining the amount of solvent absorbed at equilibrium swelling by a non-ionic crosslinked network are the crosslink density and the extent of polymer-solvent interaction, which is reported as the value of Flory-Huggins parameter χ.[22,23] The diffusion into solid samples depends on the availability of appropriate molecular size holes in the network, however it may be noted that the kinetic response which includes solvent sorption rate, the rate of approach to equilibrium and the transport mechanism controlling the solvent sorption may also depend upon additional factors like history of the samples and its composition.[24,25] The molecular weight between cross-links (M_c) was estimated using the following relation, based on the theory initially proposed by Flory and Rehner.[26]

$$\bar{M}_c = -V_1 \rho_p \frac{\varphi_p^{1/3} - 1/2\varphi_p}{\ln(1-\varphi_p) + \varphi_p + \chi\varphi_p^2} \tag{3}$$

where, V_1 is the molar volume of the solvent, ρ_p is the polymer density; φ_p is the volume fraction of the polymer in the swollen matrix, and χ is the Flory–Huggins interaction parameter between solvent and polymer, which can be calculated using following relation

$$\chi = \beta + \frac{V_1}{RT}(\delta_s - \delta_p)^2 \tag{4}$$

where δ_s and δ_p are the solubility parameters of the solvent, and the polymer β is lattice constant, R is the universal gas constant, and T is absolute temperature. The variation in crosslinking density with radiation dose for nano-composites is plotted in Figure 4. It is clear from the figure that though at lower doses there is not much difference among the crosslink densities of different nano-composites it becomes significant at higher radiation doses. The gel content attains a plateau with increasing radiation dose whereas; crosslinking density keeps increasing due to further increase in

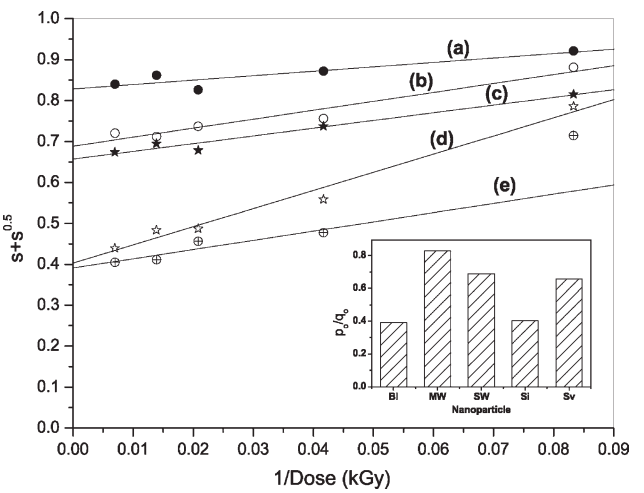

Figure 3 Charlesby-Pinner plots for PVA-nano-composites (a) MWNT, (b) SWNT, (c) Silver, (d) Silica, and (e) Blank. Inset: p_0/q_0 values for PVA-nano-composites on irradiation at a dose rate of 3.5 $kGyh^{-1}$.

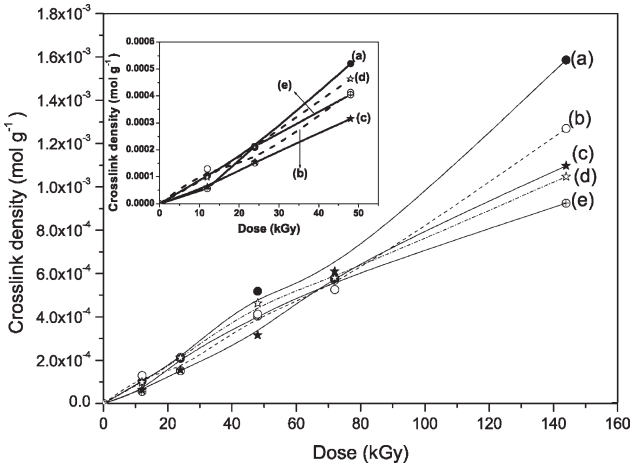

Figure 4 Crosslinking densities of PVA-nano-composites on irradiation at a dose rate of 3.5 kGyh^{-1} (a) Blank, (b) Silica, (c) Silver, (d) SWNT, and (e) MWNT; Inset: Crosslinking densities at lower radiation doses (a) Blank, (b) Silica, (c) Silver, (d) SWNT, and (e) MWNT.

intermolecular radical–radical combinations and other rearrangements. Nevertheless, crosslinking density values followed the order Bl > Si > Sv > SWNT > MWNT, in the complete dose range studied, indicating predominantly crosslinking behavior of nano-composites on irradiation and reduction in the crosslinking density with the incorporation of nano-particulate fillers.

Spectroscopic studies of nano-composites

Raman spectroscopy has been extensively used to characterize carbon nanotubes[27,28] and also to investigate its interaction with polymer matrix.[29] Particular attention has been given to radial breathing modes (RBM), which is related to the diameter of the nanotube and the tangential stretching G-bands. Therefore Raman studies of the nanocomposites were carried out to investigate the interaction between the nano-fillers and PVA. The Raman spectra of PVA containing different nano-particulate fillers have been shown in Figure 5. In the region 100–1800 cm^{-1}, only the strong modes of the PVA were clearly observed in the Raman spectra of the both SWNT-PVA and MWNT-PVA along with the modes of CNT. The Raman spectra of SWNT-PVA, MWNT-PVA composites show noticeable changes compared to pristine CNT. Pure SWNT spectrum showed G-band at 1593 cm^{-1}, D-band at 1340 cm^{-1}, whereas the G-band and D-band for SWNT-PVA nano-composite were found to be at 1631 and 1342 cm^{-1} respectively, with not much difference in their relative intensities. The D-band to G-band intensity ratios for pure SWNT and PVA-SWNT nano-composites were nearly same, indicating there is no change in the defects or disorder levels of SWNT on nano-composite formation, i.e., minor change in graphene structure of the basic structure of C-tubes. The second region of Raman spectra (2800–3000 cm^{-1}) of PVA-nano-composites due to CH stretching vibrational modes is shown in Figure 6.

Dilute solution viscometry

Figure 7 represents the variation of specific viscosity with concentration and Figure 8 shows the intrinsic viscosity values and the values of Huggins slope coefficient "b" which indicates the overall thermodynamics of the system.[30] It is clear that pure PVA has the lowest hydrodynamic volume in solution; whereas, it is the highest for its MWNT nano-composites. It clearly shows that the addition of nano-particulate fillers markedly affects polymer coil dimensions as well as the thermodynamic stability of the macromolecular complex.

Contact angle measurements

To measure the change in the hydrophilicity of the parent PVA matrix on the introduction of nano-

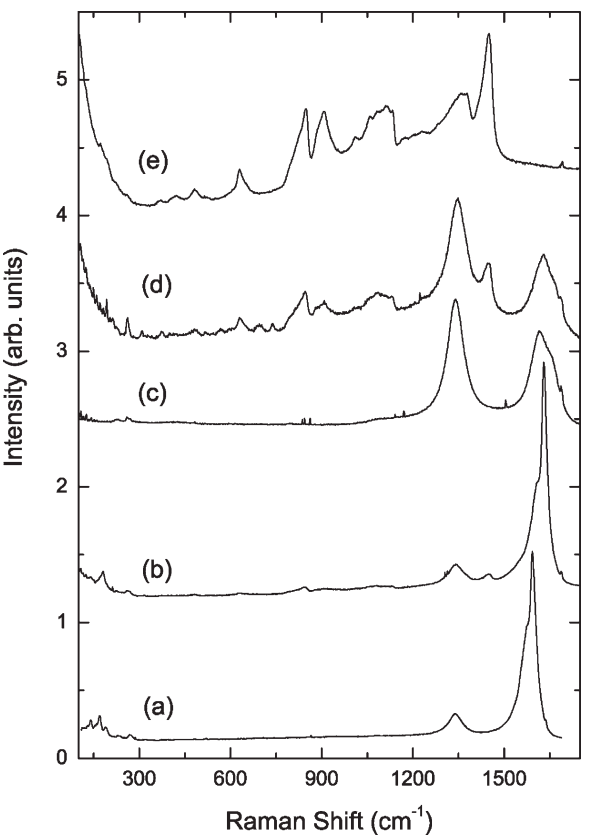

Figure 5 Raman spectra in 100–1800 cm^{-1} range of (a) SWNT, (b) PVA-SWNT, (c) MWNT, (d) PVA-MWNT, and (e) PVA.

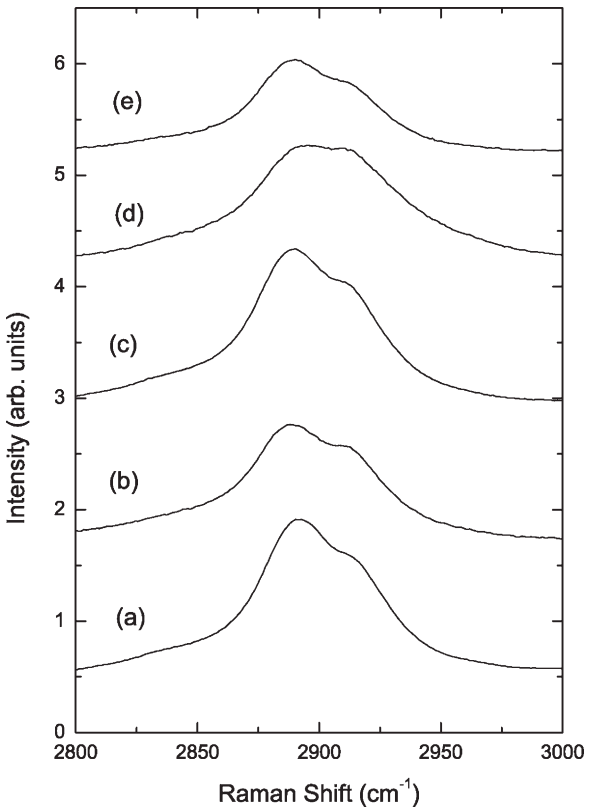

Figure 6 Raman spectra in the CH stretching mode region of nano-composites containing (a) PVA, (b) SWNT, (c) MWNT, (d) Silver, and (e) Si.

fillers, sessile drop method with image analysis was used to measure the contact angle of water, when the drop was allowed to fall on different nano-composite surfaces.[31] Figure 9 shows the photo images of water drops on the surfaces of nano-composites recorded immediately after the water drop was deposited on the surface of the nano-composites films irradiated to radiation dose of 25 kGy.

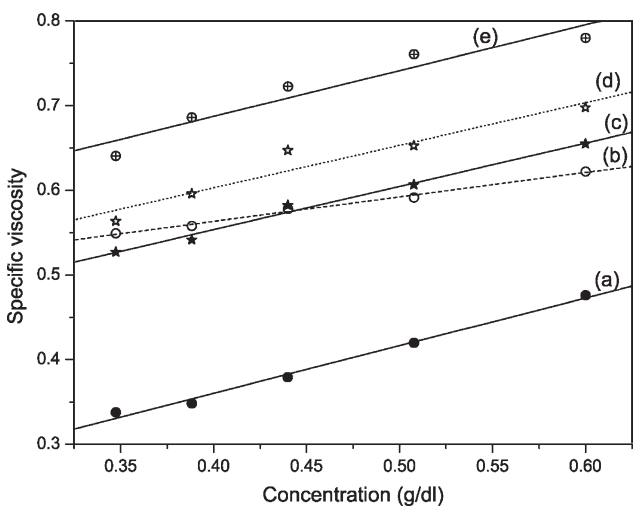

Figure 7 Viscometric profiles of PVA-nano-composites (a) Blank, (b) SWNT, (c) Silica, (d) Silver, and (e) MWNT.

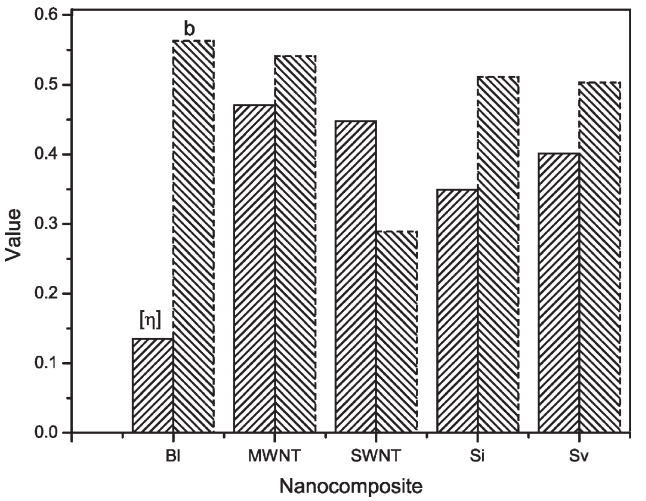

Figure 8 Intrinsic viscocity [η] and "b" for nano-composites.

DISCUSSION

Lower values of p_o/q_o for all the nano-composites are suggestive of relatively poor radical–radical interactions in polymer nano-composites and/or possible radical quenching action of nano-particulate fillers. It may be pointed out that this observation is very different from the findings of EVA/MWNT system that we have recently reported where presence of MWNT was found to increase the crosslinking extent of parent EVA matrix.[32] In the present system as the irradiation was carried out in aqueous solution, contribution due to free-volume effect observed in EVA/MWNT system may be negligible but aqueous radiation chemistry is expected to play an important role. On carefully analyzing the cross-linking inhibition sequence, the lower radiation sensitivities of nanotubes containing nano-composites (both MWNT and SWNT) than those of spherical nanoparticles (silica and silver) are quite apparent. Since, the radical–radical overlapping is mainly governed by geometrical constraints, this observation can be explained on the basis of the differences in the steric hindrances posed by overall hydrodynamic volume of nanoparticles and their interactions with PVA. Though diameter of nanotubes and nanoparticles are comparable, the overall hydrodynamic volumes of nanotubes are much higher which will lead to poor radical–radical recombination yielding lower gel fraction. A plausible explanation lies in the difference in the macromolecular dynamics of their sonicated suspensions. It is reported that agglomeration of SWNT leads to oriented bundles whereas MWNT are like entangled ropes.[7] Raman results of the nano-composites show changes in D-band and radial breathing mode of SWNT due to changes in vibration modes of bundles. Considering its better dispersion coupled with its higher surface

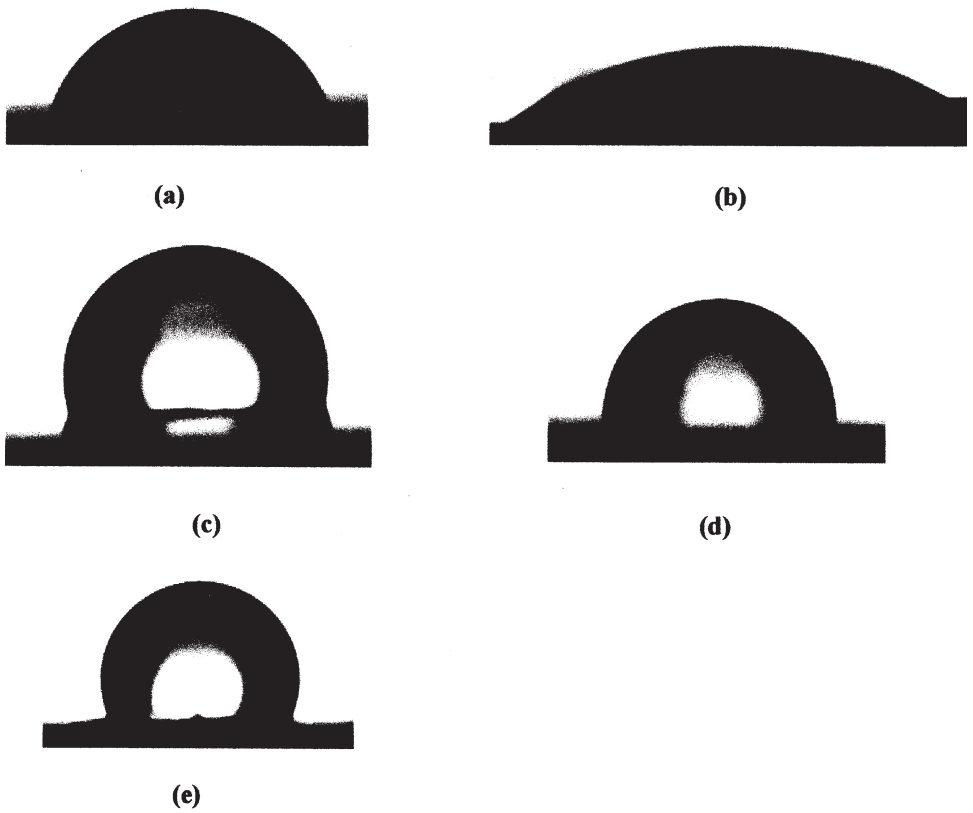

Figure 9 Water drop images on different PVA-nano-composites irradiated to a dose of 25 kGy immediately after drop was allowed to fall on nano-composite surfaces containing (a) Blank, (b) Silica, (c) Silver, (d) SWNT, and (e) MWNT.

area and lesser diameter, it can be assumed that SWNT will inhibit the radical–radical interaction to a lesser extent thereby producing relatively higher gel content.

The additives like nano-particulate fillers are expected to induce a diminishing effect of radiation, as additives absorb part of energy deposited during irradiation. Furthermore, fillers may scavenge the radicals generated on the polymer matrix, this may hinder the radical–radical interactions and reduce overall crosslinking density and gel fraction. Studies have shown that rate of radiation induced polymerization decreases in presence of inorganic fillers though the kinetics remains unchanged.[22,25,32] For aqueous polymer system, though the radiolytic products of water are generated at millimolar concentration, it has been established that net effect of radiation is due to indirect effect of these radiolytic products of water.[33] The active concentration of nano-particulate fillers like carbon nanotubes, if distributed uniformly, are expected to present in the significantly higher concentration than the concentration of radicals generated due to radiolysis of water. If the nano-filler effectively quenches the radicals generated from water or if it leads to any other radical quenching pathways, the effect of irradiation will be reduced. Therefore, the reduction in the crosslinking yield after the nano-particulate filler incorporation indicates the quenching of radicals or/and formation of lower density spurs inhibiting radical–radical recombination.[34]

In Raman spectroscopy studies, the major shift in radial breathing mode from 170 to 192 cm^{-1} could be attributed to the unbundling of SWNT and other the micro-structural changes taking place in the vicinity of carbon nanotubes surface as reported for other SWNT system. This is corroborated by the fact that radial breathing feature of SWNT might shift to higher frequencies upon their being incorporated into a polymeric matrix via a dispersion-curing procedure. There is also a possibility of bonding/interaction between the CNT and the polymer via hydrogen bonds.[27] The D-band attributed to the defects and disorder-induced modes of MWNT at 1341 and G-band at 1616 cm^{-1}, which is related to the graphite tangential E_{2g} Raman active mode (where the two atoms in graphene unit cell are vibrating tangentially one against the other), were clearly observed for both pristine MWNT and PVA-MWNT composites. However, their peak position (1347 and 1626 cm^{-1}, respectively, in MWNT-PVA) and relative intensity was found to be different in the presence of PVA. The D-band to G-band intensity ratios for pure MWNT and PVA-MWNT nanocomposites was 1.3 and 1.8, respectively, indicating the increase in the defects and disorder levels of

MWNT on nano-composite formation. Interestingly, all these characteristic peaks of MWNT, SWNT, and PVA diminished in PVA-nano-composites indicating strong interfacial interaction between PVA and nano-tube surfaces and a possibility of energy transfer between tubes and polymers. Since there is no covalent bond formation in PVA-nano-composites, the interfacial layer, in such a physical mixture is expected to be only of few nanometers. However, the strong hydrogen-bonding network of PVA is not expected to completely encapsulate the tube surfaces due to the random defects on the tube surface. The C—H and OH bending bands at 1450 cm^{-1} of the PVA appear at nearly same frequency in corresponding MWNT and SWNT composites, respectively. The bands at 1145 cm^{-1}, assigned to C—C and CO stretching vibration in the pure PVA, appear with much weaker intensity in MWNT and SWNT nano-composites. While there is a marginal change in the D-band frequency, there is a blue shift of the G-band in SWNT-PVA by about 40 cm^{-1} and in MWNT-PVA by about 10 cm^{-1} which could be either due to stress on the CNTs or bonding between the polymer and the CNTs.[29] But the shift in frequency is much higher than would be expected due to pressure from the polymer. Thus the blue shift of the tangential mode of the CNTs in the polymer composite indicates some bonding/interaction between the CNTs and the polymer.

The bands at 2891 and 2918 cm^{-1} were assigned to be the CH stretching vibration of the CH_2 in the PVA spectrum and PVA nano-composites of SWNT, MWNT, silica nanoparticles, and silver nanoparticles. Except silver-PVA nano-composites, other nano-composites did not show much change in the lineshape/frequency of the CH stretching modes. In the case of silver-PVA composites, the width of the CH mode is found to increase compared to pristine PVA. PVA molecules consist of polymer chains containing inter/intra chain hydrogen bonding; therefore addition of nano-particulate fillers may affect the extent of hydrogen bonding, crystallinity as well as the conformation of polymer chains. However from the Raman studies, it appears that hydrogen bond strength is not affected on incorporation of nano-fillers.

The lower hydrodynamic volume in DSV studies of pure PVA typifies higher coil density and provides a plausible explanation for the higher crosslinking efficiency of pure PVA. These findings also suggest that the conformational arrangements of PVA chains in nanocomposites are very different from those of pure PVA. The Huggins slope coefficient did not show much variation. Such an observation supports the Raman spectroscopy results signifying not much change in the hydrogen-bonding network both in liquid as well as in solid state. These findings indicate that nano-particulate fillers are just physically trapped inside the polymer chains, increasing the coil dimensions and adversely affecting radical interaction possibility. However, it will be erroneous to draw a direct correlation between viscosity results and gel fraction values, as the viscosity is among the various other factors that contribute to radiation crosslinking.[12,35] In the present system, along with the conformational changes in the PVA chains, nanoparticulate fillers, and the reactivity of individual nano-particulate fillers/macromolecular complex with the water radiolysis products ($^{\bullet}OH$, e^{-}_{aq} and $H^{\bullet}$) can play a critical role in radiation crosslinking. Our earlier study has shown marked dependence of gel fraction of PVA on the initial mode of radical decay.[36] Therefore, it would be worthwhile to understand the reaction of various nano-particulate fillers with water radiolysis products before attributing any of the three as predominant cause for variation in the radiation sensitivity of parent PVA matrix in presence of nano-fillers.

On comparing the initial contact angle values, it is clear that hydrophilicity of the PVA matrix is significantly affected only on introduction of silica into the matrix. In fact the hydrophilicity of PVA-silica nanocomposite is much higher than parent PVA.

CONCLUSIONS

Gel fraction, crosslinking density, and Charleby-Pinner parameter for the PVA nano-composites containing different nano-particulate fillers indicated lower radiation sensitivity of nano-composites than that of pristine PVA. The hydrodynamic volume was found to be largest with the nanotubes type nano-particulate filler than those of spherical nanoparticles. Both gel fraction and crosslinking density values followed the order Blank > Silica > Silver > SWNT > MWNT, over the entire dose range of study, indicating predominantly crosslinking behavior of nano-composites on irradiation and reduction in the crosslinking density with the incorporation of nano-particulate fillers. This was attributed to the reduced probability of spur overlap due to the formation of lower density spurs in nano-composites.

References

1. Paranhos, C. M.; Soares, B. G.; Oliveira, R. N.; Pessan, L. A. Macromol Mater Eng 2007, 292, 620.
2. Qian, D.; Dickey, E. C.; Andrews, R.; Rantell, T. Appl Phys Lett 2000, 76, 2868.
3. Song, Y. S. e-Polymers 2007, no. 047.
4. Pinnavaia, T. J.; Beall, G. W. Polymer Nano-Composites; Wiley: London, 2000; p 27.
5. Touati, N.; Kaci, M.; Ahouari, H.; Bruzuad, S.; Grohens, Y. Macromol Mater Eng 2007, 292, 1271.
6. Nejad, S. H.; Ahmadi, S. J.; Abolghasemi, H.; Mohaddespour, A. e-Polymers 2007, no. 126.

7. Wach, R. A.; Mitomo, H.; Yoshii, F.; Kume, T. Macromol Mater Eng 2002, 287, 285.
8. Dubey, K. A.; Pujari, P. K.; Ramnani, S. P.; Kadam, R. M.; Sabharwal, S. Radiat Phys Chem 2004, 69, 395.
9. Chaudhari, C. V.; Dubey, K. A.; Bhardwaj, Y. K.; Virendra, K.; Goel, N. K.; Sabharwal, S. J Radioanal Nucl Chem 2008, 278, 47.
10. Chaudhari, C. V.; Bhardwaj, Y. K.; Patil, N. D.; Dubey, K. A.; Virendra, K.; Sabharwal, S. Radiat Phys Chem 2005, 72, 613.
11. Dubey, K. A.; Bhardwaj, Y. K.; Chaudhari, C. V.; Sabharwal, S. J Appl Polym Sci 2006, 99, 3638.
12. Korolev, G. V.; Bubnova, M. L. e-Polymers 2002, no. 030.
13. Lewandowska, K. Eur Polym J 2005, 41, 55.
14. Ramaraj, B. J Appl Polym Sci 2007, 103, 1127.
15. Zhang, J.; Chen, H.; Li, P.; Wang, A. Macromol Mater Eng 2006, 291, 1529.
16. Abd El-Mohdy, H. L. J Appl Polym Sci 2007, 104, 504.
17. Zhang, W.; Chen, D.; Zhao, Q.; Fang, Y. Polymer 2003, 44, 7953.
18. Leskovac, M.; Kovačević, V.; Blagojević, L. C.; Vrsaljko, D.; Volovšek, V. e-Polymers 2004,
19. Sharifa, J.; Yunusa, W. M. Z. M.; Dahlan, K. Z. H. M.; Ahmed, M. H. Polym Test 2005, 24, 211.
20. Chapiro, A. Radiation Chemistry of Polymeric Systems; Wiley: London, 1962; p 339.
21. Woods, R. J.; Pikaev, A. K. Applied Radiation Chemistry: Radiation Processing; Wiley: New York, 1993; p 341.
22. Kuzminskii, A. S.; Nikitina, T. S.; Karpov, V. L. J. Nucl Energy 1957, 4, 268.
23. Hildenbrand, J. H.; Scott, R. L. The solubility of Non-Electrolytes, 3rd ed.; Reinhold: New York, 1949; p 93.
24. Flory, P. J. Principles of Polymer Chemistry; Cornell University Press: Ithaca, New York, 1953; p 495.
25. Stern, S. A.; Frisch, H. L. Anal Rev Mater Sci 1981, 11, 523.
26. Flory, P. J.; Rehner, R. J Chem Phys 1943, 11, 521.
27. Rao, A. M.; Richter, E.; Bandow, S.; Chase, B.; Eklund, P. C.; Williams, K. W.; Menon, M.; Subbaswamy, K. R.; Thess, A.; Smalley, R. E.; Dresselhaus, G.; Dresselhaus, M. S. Science 1997, 275, 187.
28. Rao, A. M.; Jorio, A.; Pimenta, M. A.; Dantas, M. S. S.; Saito, R.; Dresselhaus, G.; Dresselhaus, M. S. Phys Rev Lett 2000, 84, 1820.
29. Owens, F. J. J Mater Chem 2006, 16, 505.
30. Barsbay, M.; Guner, A. J Appl Polym Sci 2006, 100, 4587.
31. Cheng-Ho, C.; Fang-Yu, W.; Ching-Feng, M.; Chien-Hsin, Y. J Appl Polym Sci 2007, 105, 1086.
32. Dubey, K. A.; Bhardwaj, Y. K.; Chaudhari, C. V.; Virendra, K.; Goel, N. K.; Sabharwal, S. Express Polym Lett 2009, 3, 492.
33. Clough, R. L. Nucl Instrum Methods B 2001, 185, 8.
34. Zagorski, Z. P. Radiat Phys Chem 2002, 63, 9.
35. Dubey, K. A.; Bhardwaj, Y. K.; Chaudhari, C. V.; Virendra, K.; Goel, N. K.; Sabharwal, S. J Appl Polym Sci 2009, 111, 1884.
36. Dubey, K. A.; Bhardwaj, Y. K.; Chaudhari, C. V.; Sabharwal, S.; Mohan, H. React Funct Polym 2007, 67, 282.